PNAS RESEARCH ARTICLE | EVOLUTION

Phylogenomics of the tetraploid Hawaiian lobeliads: Implications for their origin, dispersal history, and adaptive radiation

Jeffrey P. Rose[a,1], Bing Li[a], Margaret J. Sporck-Koehler[b], Elizabeth A. Stacy[c], Kenneth R. Wood[d], Emily Moriarty Lemmon[e], Alan R. Lemmon[f], Cécile Ané[a,g], Kenneth J. Sytsma[a], and Thomas J. Givnish[a]

Affiliations are included on p. 11.

Edited by Loren Rieseberg, The University of British Columbia, Vancouver, BC, Canada; received October 14, 2024; accepted March 26, 2025

Hawaiian lobeliads exhibit extensive adaptive radiations and are considered the largest plant clade (143 species) endemic to any oceanic archipelago. Rapid insular radiations are prone to reticulate evolution, yet detecting hybridization is often limited by inadequate sampling of taxa or independent loci. We analyzed 633 nuclear loci (including tetraploid duplications) and whole plastomes for 89% of extant species to derive phylogenies for the Hawaiian lobeliads. Nuclear data provide strong support for nine major clades in both likelihood and ASTRAL analyses. All genera/sections are monophyletic except *Clermontia* and *Cyanea*. Nuclear and plastome phylogenies conflict on short, deep branches; the nuclear tree resolves a fleshy-fruited clade of Hawaiian *Clermontia/Cyanea-Brighamia/Delissea*, sister to Polynesian *Sclerotheca*, with both sister to a capsular-fruited Hawaiian clade. Incomplete lineage sorting in a rapid radiation starting 8.5–11.3 Ma is sufficient to explain uncertainty and cytonuclear discordance along the backbone. Sequence data support reticulation within *Clermontia* and especially *Cyanea*. Nuclear data identify 42 interisland dispersal events: 89% accord with the strict progression rule, involving movement to the next younger island in the hotspot chain, consistent with theory. Plastid data overestimate such events by 17%. *Cyanea* and *Clermontia* have undergone parallel adaptive radiations in elevational distribution and flower length on all major islands, with multiple founders and some interisland differences. Hawaiian lobeliad diversification was driven by an early intergeneric divergence in habitat, followed by parallel adaptive radiation and ecological speciation within *Clermontia/Cyanea*, combined with widespread single-island endemism, frequent interisland dispersal, and occasional hybridization.

adaptive radiation | disparification | ecological saturation | speciation | incomplete lineage sorting

Significance

Archipelagoes present exciting opportunities to understand the process of adaptive radiation. To better understand the roles of hybridization, geographic isolation, and trait divergence in adaptive radiation, we reconstructed relationships among 101 species of Hawaiian lobeliads using data from 633 nuclear loci and plastomes. Plastomes suggest Hawaiian lineages are monophyletic, but nuclear data place Polynesian *Sclerotheca* sister to fleshy-fruited Hawaiian genera. This conflict reflects rapid divergence rather than hybridization. We found that 89% of interisland dispersals were to the next younger and closest island. Lobeliad diversity reflects nearly parallel radiations in elevation and flower length on all major islands in the two largest genera. This highlights the crucial roles of parallel radiation, frequent interisland dispersal, and single-island endemism in diversification.

From a single ancestor that arrived in the Hawaiian archipelago 7.5 to 13.6 Ma (1, 2), the native Hawaiian lobeliads have evolved into the most species-rich plant clade in Hawaii or any other single oceanic archipelago, comprising 143 species (114 of which are extant) and thus 11.5% of all native Hawaiian angiosperms (3, 4). Native Hawaiian lobeliads are currently classified into seven clades: *Brighamia, Clermontia, Cyanea, Delissea, Lobelia* § *Galeatella* (*Galeatella*), *Lobelia* § *Revolutella* (*Revolutella*), and *Trematolobelia*. All are restricted to the eight tall Hawaiian Islands and the thirteen volcanoes forming them. The Hawaiian lobeliads have undergone spectacular radiations in habitat, means of dispersal, growth form, floral morphology, leaf shape, and photosynthetic physiology (1, 5–13). They almost certainly facilitated, via coevolution, the diversification of Hawaiian honeycreepers (Fringillidae) and honeyeaters (Mohoidae), the two largest clades of native birds, which include almost all pollinators of the Hawaiian lobeliads (14, 15), as well as the Hawaiian fruit flies (Drosophilidae), by far the largest clade of native arthropods, many of which use lobeliads as mating or oviposition sites (16, 17). Most species are restricted to single islands (mean number of islands occupied = 1.27 ± 0.71 SD) or, indeed, single volcanoes (mean = 1.57 ± 1.12 SD) (*SI Appendix*, Tables S1–S3). More than half of Hawaiian lobeliad species are threatened or endangered (35%) or considered extinct (21%) and 65% of *Cyanea* species are threatened, endangered, or extinct. These losses and looming threats to the Hawaiian lobeliads reflect habitat destruction, consumption by introduced vertebrate herbivores, loss of pollinators and seed dispersers, and competition with introduced plant species.

The origin of each of the seven genera/sections of native Hawaiian lobeliads predates the emergence of Ni'hau (1), the oldest tall island in the Hawaiian-Emperor seamount chain (18, 19). Biogeographic analyses of a subsample of species indicate that as the Hawaiian island chain grew, colonists in at least *Cyanea* and *Clermontia* (1, 11) dispersed largely in accord with the progression rule (20, 21)—from one island onto the nearest

Author contributions: J.P.R., K.J.S., and T.J.G. designed research; J.P.R., B.L., E.M.L., and A.R.L. performed research; E.M.L., A.R.L., and C.A. contributed new reagents/analytic tools; J.P.R., B.L., E.M.L., A.R.L., C.A., and T.J.G. analyzed data; M.J.S.-K., E.A.S., and K.R.W. provided samples; and J.P.R., B.L., and T.J.G. wrote the paper.

The authors declare no competing interest.

This article is a PNAS Direct Submission.

[1]To whom correspondence may be addressed. Email: rose.873@osu.edu.

This article contains supporting information online at https://www.pnas.org/lookup/suppl/doi:10.1073/pnas.2421004122/-/DCSupplemental.

Published May 5, 2025.

younger, ecologically unsaturated island immediately to the southeast—in agreement with theory and patterns observed in other Hawaiian lineages (22–27). Extinction and incomplete sampling might lend false support for the progression rule. The first is difficult or impossible to account for, but the second can be ameliorated by thorough sampling. At least *Cyanea* appears to have undergone parallel adaptive radiation in elevational distribution and flower tube length on each of the four major islands or island groups (Kaua'i [Kaua'i and Ni'ihau], O'ahu, Maui Nui [Lāna'i, Maui, and Moloka'i], and Hawai'i). Divergence along these axes of variation are critical components of reproductive isolation via differences in pollinator and microhabitat, promoting ecological speciation and coexistence among closely related species (1). However, previous analyses left unresolved the relationships among *Cyanea* species within islands, how many founders seeded radiations on each island, and the extent to which radiations are actually parallel and contribute to the overall diversification of the Hawaiian lobeliads. Such questions are crucial for understanding the adaptive radiation and species diversification not only of the Hawaiian lobeliads, but of other large lineages on hotspot archipelagoes worldwide.

The initial, rapid radiation of all Hawaiian genera/sections appears tied to divergence in habitat, with berry-fruited *Cyanea* and *Clermontia* mostly restricted to wet forest interiors, canopies, and edges; berry-fruited *Delissea*, to mesic scrub; capsular-fruited *Brighamia*, to sea cliffs; capsular-fruited *Galeatella*, to mostly alpine bogs; capsular-fruited *Revolutella* to interior rock walls; and capsular-fruited *Trematolobelia*, to openings in wet, high-elevation forests and bog edges (1). Hawaiian lobeliads with wind-dispersed seeds generally occur in open habitats and those with bird-dispersed seeds in more closed habitats (1).

Our understanding of gene flow, dispersal, and adaptive radiation in the Hawaiian lobeliads remains incompletely understood, given that previous analyses excluded over half the extant species and were based almost entirely on plastid sequences. The latter is problematic because plastid capture among closely related species on the same island might mask the presence of relatively unrelated nuclear clades on either the source or target islands, obscuring independent dispersal events. Accounting for reticulate evolution in studies of interisland dispersal in Hawaiian plant lineages apart from a simple comparison of gene-tree topologies is still in its infancy, yet a consideration of reticulate evolution due to hybridization or introgression is a crucial issue for many Hawaiian plant lineages due to the co-occurrence of recently divergent species on individual islands. Recent efforts using multilocus or genome-level datasets to better resolve relationships within lineages of Hawaiian plants (26, 28–32) show strong evidence for reticulate evolution within recent and rapid radiations, but none have investigated the differential causes of cytonuclear discordance while sampling hundreds of nuclear loci and the vast majority of extant species diversity to obtain comprehensive views of biogeographic history and adaptive radiation.

Previous phylogenetic studies of the Hawaiian lobeliads—except those focused on *Cyanea* (7, 8) and *Clermontia* (11, 33)—have been based on sampling of less (or far less) than half of all extant species. However, they have established that the major clades of Hawaiian lobeliads are monophyletic (1, 7, 8, 34) except for *Clermontia* and *Cyanea* (11, 33–36), and that there is strong support for the sister clades of *Brighamia*/*Delissea*, *Galeatella*/*Trematolobelia*, and *Clermontia*/*Cyanea*. Relationships among these three broader groups, *Revolutella*, and certain non-Hawaiian taxa (e.g., Polynesian *Sclerotheca*) have not been resolved consistently or conclusively across studies (1, 7, 8, 34, 35), nor has there been consensus on the closest relatives of the Hawaiian lobeliads (1, 2, 36–38). Moreover, signals of hybridization or introgression are unexplored except for *Clermontia* (11), where five potential hybrid species were identified based on cytonuclear incongruence.

Here, we reexamine the evolutionary relationships among species and major clades of the Hawaiian lobeliads, using sequence data generated from anchored hybrid enrichment of 633 nuclear loci and plastomes for 89% of extant species. We use these data to infer phylogenetic relationships and screen for the relative importance of incomplete lineage sorting (ILS) and hybridization. We calibrate these phylogenies against time to infer the history of interisland dispersals and speciation within islands. Finally, we quantify and compare adaptive radiation in elevational distribution and flower tube length across clades and islands, focusing on the two largest genera, *Cyanea* and *Clermontia*. We ask whether closely related species on the same island differ in elevation or flower size (presumably due to divergent selection to reduce competition and/or mismating) and evaluate the extent to which within-island radiations in *Cyanea* and *Clermontia* are indeed parallel, are seeded by multiple founders, and contribute to species diversification of the Hawaiian lobeliads.

Results

Molecular Phylogenies. We conducted four series of phylogenetic analyses to estimate 1) nuclear trees based on 633 loci, 2) plastome trees based on exons or nearly complete genomes, 3) nuclear and plastome trees calibrated to absolute time, and 4) phylogenetic networks including representatives of all major ingroup clades.

Nuclear Trees. Both maximum likelihood (ML) and ASTRAL analyses of 633 nuclear loci recovered the same relationship among the eight major ingroups (*Brighamia*, *Delissea, Clermontia, Cyanea*, *Galeatella*, *Revolutella*, *Sclerotheca*, *Trematolobelia*) with varying levels of support (Fig. 1*A* and *SI Appendix*, Figs. S1–S3). The monophyly of all ingroups received maximal support, except for *Cyanea* and *Clermontia*. There is strong support for the paraphyly of *Cyanea*, with the orange-fruited (OF) clade containing species that almost all bear orange fruits sister to the clade formed by *Clermontia* plus the purple-fruited (PF) clade containing species of *Cyanea* that almost all bear purple fruits (bootstrap support [BS] = 100, local posterior probability [LPP] > 0.99). *Clermontia* is not monophyletic, with *Cl. pyrularia* nested in PF *Cyanea* in each species tree and sister to or nested within one or both clades of *Cyanea* in 99% of rootable gene trees. Sister relationships of *Brighamia*/*Delissea* and *Trematolobelia*/*Galeatella* were also recovered with maximal support. Monophyly of *Trematolobelia*/*Galeatella*/*Revolutella* was well supported in the ML tree (BS = 99), but poorly supported in the ASTRAL topology (LPP = 0.37).

Apart from these well-supported relationships, there is considerable uncertainty regarding the deepest relationships of Hawaiian lobeliads and *Sclerotheca* (Fig. 2*A*). While both ASTRAL and ML topologies have identical backbone topologies, ASTRAL support is low for three critical nodes involving the placement of *Brighamia*/*Delissea*, *Sclerotheca*, and *Revolutella*. On the other hand, ML support is high (>97% BS) for all nodes except the placement of *Brighamia*/*Delissea* (71% BS) (Fig. 1 and *SI Appendix*, Figs. S1–S3). Neither ML nor ASTRAL analyses of the nuclear data recover the Hawaiian lobeliads as monophyletic, and instead find weak support for *Sclerotheca* nested within the Hawaiian lineage. Our nuclear trees indicate the emergence of a fleshy-fruited clade in mesic and wet forests (*Brighamia*/*Delissea*-*Cyanea*/*Clermontia*) (capsular fruits form late in development in cliff-dwelling

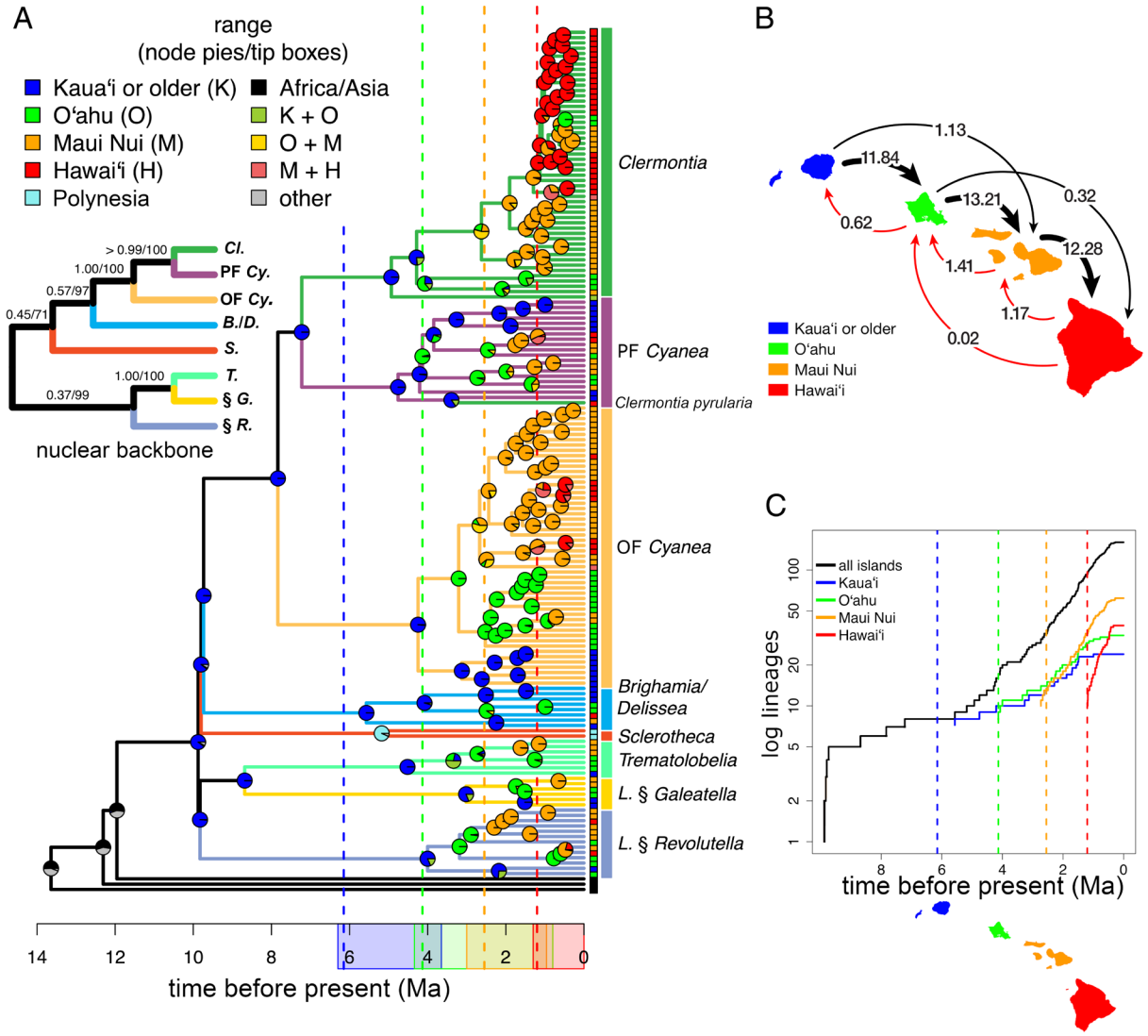

Fig. 1. Nuclear phylogenetic tree and historical biogeography. (*A*) Ancestral range estimation. Branch lengths are based on substitutions/site calibrated to absolute time, with a cladogram of backbone relationships shown at the Upper *Left*, with node labels displaying ASTRAL local posterior probabilities followed by maximum likelihood bootstrap support. Branches and rightmost tip boxes are colored by major clade, with leftmost tip boxes showing present-day ranges. Dashed vertical lines depict mean ages of island emergence and colored boxes encompass the estimated extent of the growth phase of each island, including uncertainty. (*B*) Mean number of dispersal events between islands. Thin black lines accord with a relaxed progression rule, thick black lines align with a strict progression rule, and red lines show violations of a progression rule. (*C*) Lineage-through-time plots for individual islands. Dashed vertical lines depict mean ages of island emergence.

Brighamia) from a paraphyletic capsular-fruited lineage from more open habitats (*Sclerotheca*, then *Revolutella*/*Trematolobelia*/*Galeatella*, then *Lobelia* generally). The nuclear phylogeny also implies a shift from terminal to axillary inflorescences, with terminal inflorescences in *Revolutella*/*Trematolobelia*/*Galeatella* and *Lobelia* generally, and the evolution of axillary inflorescences in fleshy-fruited Hawaiian species + *Sclerotheca*. Relationships within clades are well supported and congruent except within *Clermontia* and OF *Cyanea*, where several clades (including some older ones), are poorly supported and/or conflict between the ASTRAL and ML topologies (*SI Appendix*, Figs. S1–S3). Branch lengths deep in the nuclear phylogeny are exceptionally short, with the fleshy-fruited clade, *Sclerotheca*, and *Revolutella*/*Trematolobelia*/*Galeatella* forming a near trichotomy. The Hawaiian, Polynesian, Bonin Island, Africa, and Asian woody lobeliads appear to have diverged from each other ~12 to 14 Mya (Fig. 1*A*).

Plastome Relationships. Backbone relationships in our genealogies based on exons or nearly complete plastomes (Fig. 2*B* and *SI Appendix*, Figs. S4 and S5) are consistent with previous results (1, 2, 38). *Sclerotheca* is sister to monophyletic Hawaiian lobeliads (BS = 98 in both datasets). All other ingroup relationships are consistent with those found based on nuclear data and strongly supported except for the sister relationship between *Brighamia*/*Delissea* and *Trematolobelia*/*Galeatella*/*Revolutella* (exon BS = 100, plastome BS = 75). As with the nuclear phylogeny, there is considerable uncertainty along the backbones of *Clermontia* and OF *Cyanea* in both phylogenies based on plastid sequences.

Nuclear Backbone Discordance. Analysis of gene trees shows strong support for all nine major clades recovered in the nuclear ASTRAL and ML trees (Fig. 2*A*), with at least 263 gene trees supporting (BS ≥ 95) the monophyly of these genera/sections (mean = 390 ± 140 SD). Conversely, few gene trees support the monophyly of any recovered backbone clade or alternative resolution.

Network analyses across 10 subsets of randomly pruned gene trees favored one hybridization event (h = 1) for eight datasets and h = 2 for two datasets (*SI Appendix*, Fig. S6). Networks for h = 1 suggested intergeneric gene flow between *Brighamia*

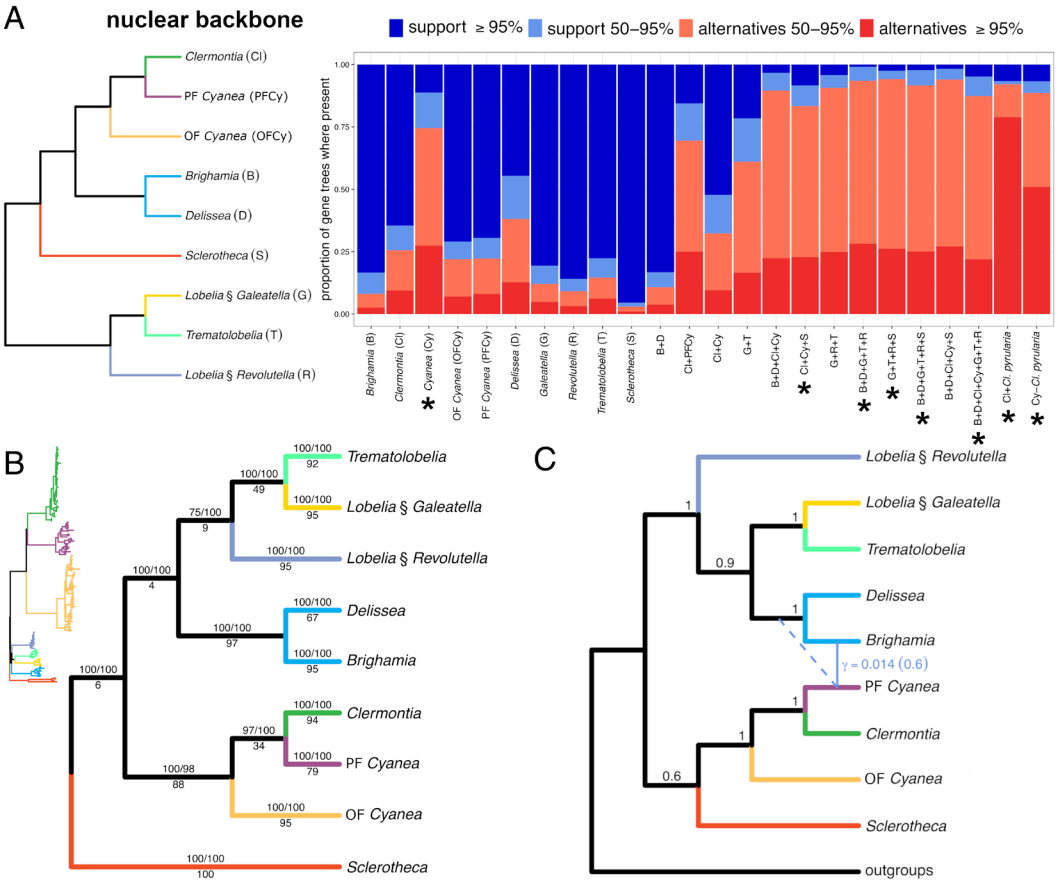

Fig. 2. Patterns of genomic discordance. (*A*) Proportion of nuclear gene trees supporting or conflicting major clades. Clades marked with an asterisk (*) conflict with the nuclear species tree topology, shown at *Left*. (*B*) Backbone of the plastome genealogy. A phylogram with branches colored by major clade is at the *Upper Left*. Node labels above branches are maximum likelihood bootstrap support in the order of plastome/exon only datasets. Node labels below branches are percent bipartition support based on coalescent gene trees simulated on the nuclear species tree. (*C*) Summary phylogenetic network from 10 sets of randomly pruned nuclear gene trees.

(possibly also involving *Delissea*) and PF *Cyanea* (possibly also involving *Clermontia*) but estimates of the proportion of the genome exchanged (γ) are 0.5 to 1.5% (Fig. 2*C* and *SI Appendix*, Fig. S6), largely rejecting the hypothesis that any conflict along the backbone is due to ancient gene flow. All 10 networks suggested a major topology different from the other nuclear and plastid topologies, although most are consistent with the latter.

Discordance within and among Genomes. Based on simulated nuclear trees (*Materials and Methods*) the deepest conflicting splits between the nuclear and plastome topologies—involving the placements of *Brighamia/Delissea* and *Sclerotheca*—received ASTRAL LPP = 0 (*SI Appendix*, Fig. S7). This is because within the simulated nuclear trees, quadripartitions from the plastome topology are less frequent than their second alternative resolution. However, plastid quadripartitions still show up at ~30% frequency. A small proportion of simulated nuclear gene trees supports the discordant plastid bipartitions of monophyletic Hawaiian lobeliads (6%), *Brighamia/Delissea/Trematolobelia/Galeatella/Revolutella* (4%), and *Trematolobelia/Galeatella/Revolutella* (9%) (Fig. 2*C*).

At shallower scales, cytonuclear discordance is almost nonexistent outside of *Clermontia/Cyanea* except within a few species of *Revolutella* (*SI Appendix*, Fig. S8). While many plastid clades within *Clermontia* and *Cyanea* are consistent with the nuclear tree under ILS, some are not, especially along the backbones of *Clermontia*, PF *Cyanea* on Kaua'i, and shallower nodes in OF *Cyanea*. Conflicts in the latter may be exacerbated by phylogenetic uncertainty [e.g., see low support for many nodes in OF *Cyanea* (*SI Appendix*, Fig. S7)].

The HyDe analysis found 3,306/595,455 triplets with evidence for γ > 0. Significant pairwise comparisons are usually within, rather than between major clades, especially *Clermontia* and *Cyanea*, although interclade gene flow possibly occurred between PF/OF *Cyanea*, PF *Cyanea/Clermontia*, and/or *Galeatella/Trematolobelia* (*SI Appendix*, Figs. S9 and S10).

Historical Biogeography. Based on nuclear data, the common ancestor of Hawaiian lobeliads arose 9.88 Ma [95% highest posterior density (HPD) = 8.45 to 11.26 Ma] with the stem lineages of most genera/sections originating rapidly, with *Brighamia/Delissea* diverging most recently at 5.57 Ma (95% HPD = 3.85 to 7.34 Ma; Fig. 1*A*). By contrast the crown ages of genera/sections are relatively young, ranging from 4.93 Ma to 2.25 Ma. Based on plastid data, the crown age of Hawaiian lobeliads + *Sclerotheca* is 11.96 Ma (95% HPD = 10.81 to 13.02 Ma). There is a similar rapid divergence among plastid lineages, with crown ages of genera/sections ranging from 6.67 Ma to 1.62 Ma. MRCA ages tend to be younger from plastid than nuclear data toward the present, and older for nodes >10 Ma (*SI Appendix*, Fig. S11). Based on the nuclear genome, the accumulation of extant lineages proceeded slowly until ~5.8 Ma (Fig. 1 *A* and *B*), but only spiked for individual islands at ~2.6 Ma (O'ahu), ~2.4 Ma (Kaua'i and Maui Nui), and ~1.3 Ma (Hawai'i). Given that most lobeliad species are restricted to single islands (*SI Appendix*, Table S2), island subsidence may mislead interpretations of rates of lobeliad diversification before Kaua'i emerged (Fig. 1*C*).

Biogeographical reconstructions favor DEC+J over DEC for both nuclear (χ^2 = 52.27, df =1, P = 4.84 × 10^{-13}) and plastid (χ^2 = 35.53, df = 1, P = 2.51 × 10^{-9}) datasets (Fig. 1*A* and *SI Appendix*, Figs. S12–S15). For the nuclear tree, an average of 70% of all biogeographical events occur within the same area under DEC+J (DEC: 63%) versus 71% in the plastid tree (DEC: 66%). Based on stochastic mapping on the nuclear tree, there are an average of 43.63 ± 1.93 SD dispersal events (42 within Hawaii) under DEC+J, of which 89% conform to a strict progression rule (dispersal to the next youngest island) and 92% to a lax progression rule (dispersal to younger islands) (39: 92.9% and 93.4% for DEC) (Fig. 1*B* and *SI Appendix*, Tables S4 and S5). Based on the plastid tree, there are an average of 51.12 ± 2.09 SD dispersal events (49 within Hawaii) under DEC+J, of which 88% conform to a strict progression rule and 93% to a lax progression rule (46: 93% and 94% for DEC) (*SI Appendix*, Tables S6 and S7). Based on stochastic mapping, an average of 127.4 of 162 cladogenetic events occurred with islands. Thus, speciation within islands accounts for ~79% of species diversification, versus ~21% for interisland dispersal.

Adaptive Radiation. Hawaiian lobeliads differ somewhat in their position and variability in ecomorphospace (elevation × flower length) by clades and islands (Fig. 3 and *SI Appendix*, Figs. S16 and S17). Species within *Brighamia*, *Galeatella*, *Revolutella*, and *Trematolobelia* display limited ecomorphological divergence and thus limited variance among species, while *Delissea* has primarily diversified in elevation and varies predominantly among islands. Intergeneric/intersectional hybrids are unknown, and different clades often occur in different habitats (see above), so their overlap in ecomorphological space is not clearly relevant to reproductive isolation or resource partitioning. Species number and the ecomorphospace occupied by individual clades increase together: species-poor *Galeatella* and *Trematolobelia* occupy the least space, and species-rich OF *Cyanea*, PF *Cyanea*, and *Clermontia* the most (Fig. 3).

Species of OF *Cyanea*, PF *Cyanea*, and *Clermontia* have evolved in largely parallel manner along both axes of variation across and within all islands, but with the most diverse lineage (OF *Cyanea*) having more species with long flowers at lower elevations than PF *Cyanea* and *Clermontia* (Fig. 3). *Cyanea* species occupy forest interiors and interspecific competition on a given island is more likely than among edge- and gap-dwelling *Clermontia* species, so *Cyanea* species on each island should be likely to diverge in elevation and flower tube length to partition resources and avoid hybridization. *Cyanea* assemblages on Kaua'i, O'ahu, Maui Nui, and Hawai'i overlap with 35, 23, 67, and 51% of the ecomorphological space occupied by *Cyanea* overall (*SI Appendix*, Fig. S17). The assemblages of *Cyanea* species on Kaua'i and O'ahu show truncated ranges of elevations occupied. These islands are far shorter (1,599 and 1,220 m, respectively) than Maui or Hawai'i, so *Cyanea* species on the older islands cannot inhabit the last 530 to 910 m of elevation occupied

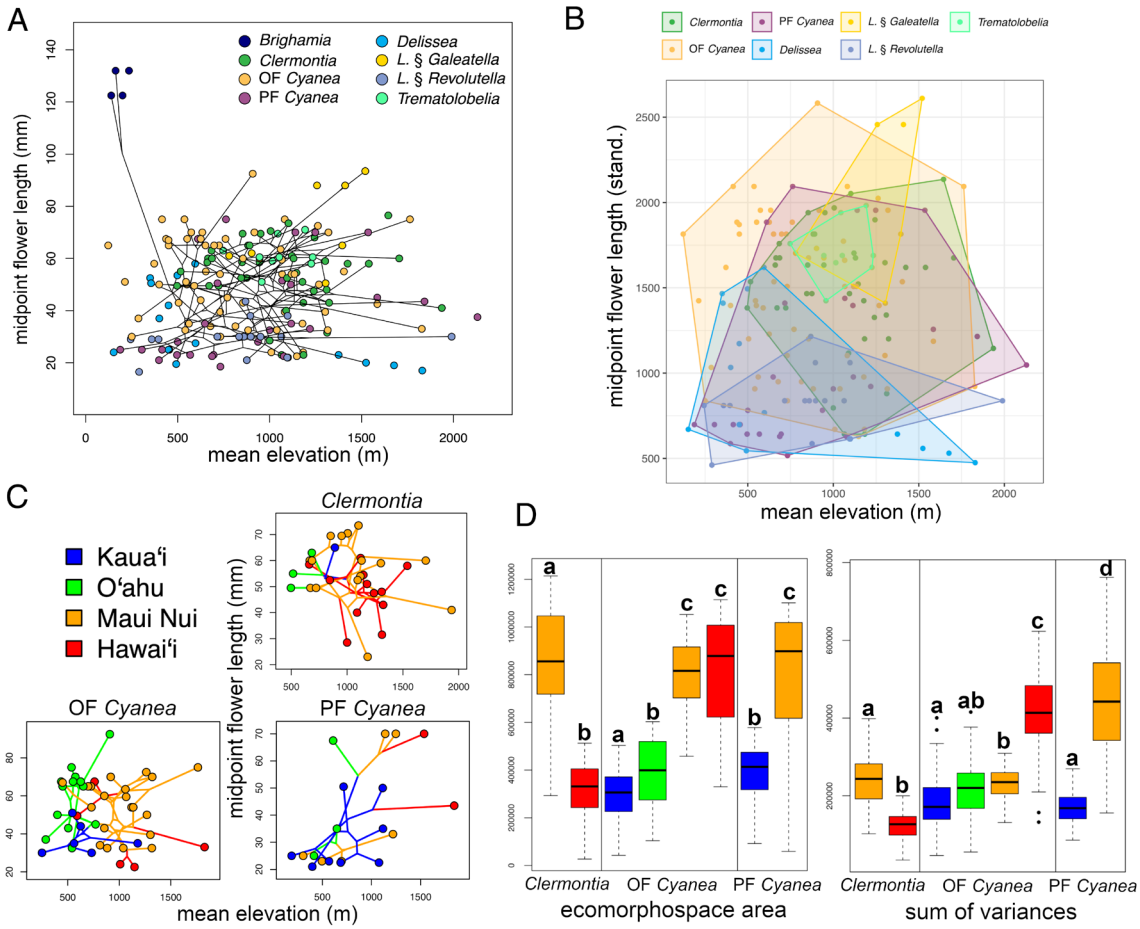

Fig. 3. Trait diversification and disparification during adaptive radiation. (*A*) Phyloecomorphospace of elevation and flower length. Each point represents a species/subspecies × island combination under a seven-island model, colored by clade. Black lines show the nuclear phylogeny superimposed on the plot. (*B*) Same as (*A*) but with minimum convex polygons drawn around points and the outlier of *Brighamia* removed. (*C*) Phyloecomorphospace plots for *Clermontia* and both clades of *Cyanea* with points and branches colored by island. (*D*) Trait disparity for *Clermontia* and *Cyanea* across islands supporting >four species per clade, including total area of ecomorphospace occupied and divergence among species within each island measured as the sum of variances. Letters denote statistically similar groups based on pairwise tests within ecological groupings (*Clermontia* and pooled *Cyanea*).

by *Cyanea* on the younger islands. Taking this limitation into account, the assemblages of *Cyanea* species on Kaua'i and O'ahu occupy 45 and 39% of the ecomorphospace occupied by the genus on these two axes. On average, assemblages on each of the four major islands occupy 50.5 ± 12.0% of the ecomorphospace available. Except for O'ahu, the ecomorphospace shared among *Cyanea* assemblages on different islands is, on average, 4.0 ± 7.2% greater if we exclude the two outlier species with unusually long flowers (92.5 mm for *C. konahuanuiensis* from O'ahu versus maximum of 75 mm otherwise) and elevations (2,130 m for *C. pohaku* from Maui versus maximum of 1,858 m otherwise). *Cyanea* species with flower tube lengths >51 mm long are missing on Kaua'i, which might reflect adaptations dependent on the history of their principal pollinators, the honeycreepers, which arose within the last 5.8 Ma and had ancestrally shorter bills (15). *Cyanea* species occupy the greatest range of elevations and flower tube lengths on Maui Nui, closely approached by the much less diverse (13 versus 24 species) assemblage on the youngest island of Hawai'i. *Cyanea* has far fewer species on Hawai'i than expected based on island area and elevation, and a lower fraction of single-island endemics (83% versus 90 to 95% on other islands), presumably reflecting its recent emergence and incomplete colonization and in situ diversification as a result (1).

While the three most species-rich clades—*Clermontia*, OF *Cyanea*, and PF *Cyanea*—occupy the greatest total amount of ecomorphospace, they do not always partition that space in precisely the same way within islands, nor do they occupy similar extents of ecomorphospace (Fig. 3). Both total ecomorphospace area occupied and variance among species varies significantly among islands (Fig. 3 and *SI Appendix*, Figs. S16–S18 and Tables S8 and S9). Within clades, assemblages on the younger islands, especially Maui Nui, occupy large areas of ecomorphospace. Variation among species in ecomorphospace, measured as the sum of variances, generally shows a similar trend as total ecomorphospace occupied, except for OF *Cyanea* on Maui Nui, where variance among species is significantly reduced compared to PF *Cyanea* on Maui Nui and OF *Cyanea* on Hawai'i, despite species on both islands occupying a similar breadth of ecomorphospace.

Although island assemblages may occupy large portions of ecomorphospace, both the range of ecomorphospace occupied and the sum of variances within an island are significantly lower than would be expected from a random sample of congeners, except for *Clermontia* and PF *Cyanea* on Maui Nui and OF *Cyanea* and pooled *Cyanea* on Hawai'i (*SI Appendix*, Figs. S19–S22), reinforcing the fact that each island radiation—especially those on older, shorter islands—occupies smaller areas of ecomorphospace than that found across the archipelago within each clade (see above and *Discussion*). Phylogenetic trait structuring within each island shows a pattern of trait divergence along one or both axes of ecomorphological space early in the history of the clade on the island, with the intervening area of ecomorphospace populated by more recent, parallel evolution (*SI Appendix*, Figs. S23–S25).

Discussion

This study provides the most extensively sampled phylogeny of a Hawaiian plant lineage to date, including more than twice as many species as any other study, and three times more than studies based on phylogenomic data. Our findings present a robust phylogenetic hypothesis for a clade comprising 11.5% of angiosperms native to the archipelago, with our sampling covering 8% of the native Hawaiian species. Of the 42 species missing from our analysis, 30 are considered extinct; most are known only from the type and often were last collected more than a century ago, making inclusion difficult or impossible at present.

Robust hypotheses of evolutionary relationships based on many independent loci and accounting for potential sources of gene tree discordance are essential for understanding the dynamic evolutionary history of the Hawaiian biota. Although Hawaii-centric studies employing hundreds or thousands of nuclear loci are multiplying (26, 28–32), current hypotheses for many Hawaiian plant clades are based on plastid or a few nuclear loci. Such analyses might be misled by artifacts caused by phylogenetic uncertainty resulting from low sequence divergence, ILS, hybridization/introgression, or plastid capture. This study therefore represents a significant advance in understanding the origin, spread, and diversification of the Hawaiian flora.

Phylogenomic Conflict along the Backbone of a Rapid Mid-Oceanic Radiation. Prior studies based on nearly complete plastomes have been unable to resolve relationships among Hawaiian lobeliad subclades or even the backbone of Lobelioideae, and thus determine their monophyly (1, 38). Our most compelling phylogeny, based on 633 single-copy nuclear loci (Fig. 1 and *SI Appendix*, Figs. S1–S3), identified a fleshy-fruited Hawaiian clade (*Clermontia*/*Cyanea*/*Brighamia*/*Delissea*) sister to *Sclerotheca*, with both sister to a capsular-fruited Hawaiian clade [*Revolutella*, (*Trematolobelia*, *Galeatella*)]. This implies one gain of axillary inflorescences (in the fleshy-fruited clade + *Sclerotheca*), one gain of fleshy fruits (in the fleshy-fruited clade), and one loss of the latter late in fruit development in *Brighamia*. Despite not finding strong support for a single bifurcating topology—with relationships of *Brighamia*/*Delissea* and *Sclerotheca* being especially problematic—we can exclude some causes for this uncertainty. Our inability to discern backbone relationships is not due to uninformative gene trees (Fig. 2). We cannot exclude ancient gene flow, but the low proportion of genome exchange between deeper lineages argues against it. The most straightforward interpretation of our data is that lobeliads diverged following their colonization of the Hawaiian-Emperor seamount chain (with subsequent dispersal to Polynesia in *Sclerotheca*) so rapidly—in 90 ka (Fig. 1) versus earlier estimates of 5 Ma (1)—that the effects of ILS on the distribution of gene trees severely impacts our ability to reconstruct its deep phylogenetic history. The Hawaiian lobeliads (including *Sclerotheca*) represent a highly challenging scenario for species tree inference. Short, deep internal branches, long terminal branches, and an imbalanced branching order result in extreme ILS in the "anomaly zone" (39–41). This problem may be further exacerbated by low substitution rates in the nuclear genomes, as observed in the plastomes of other lobeliads (1). Lineage splitting may have occurred too fast for mutations to accumulate or genes to coalescence to inform branching order. Analyses of whole-genome sequences (32) or structure are possible future avenues for conclusively resolving backbone relationships and reconstructing ancient hybridization in the Hawaiian lobeliads and their relatives.

Deep cytonuclear discordance is also best accounted for by a rapid radiation rather than organellar capture. The plastid topology can be explained as a random resolution of relationships under high ILS, as a low but not insignificant proportion of bipartitions found in simulated nuclear gene trees mirror those found in the plastome tree. Although ASTRAL LPP = 0 for these quadripartitions, even assuming that poorly supported areas of the ASTRAL tree are "true," ~30% of the conflicting quadripartitions show up in the simulated nuclear species trees (*SI Appendix*, Fig. S7).

Evidence for More Recent Introgression. Site pattern frequencies and cytonuclear discordance show clear evidence for interspecific gene flow within major clades. Our HyDe analyses are somewhat at odds with our phylogenetic network, suggesting gene flow involving all pairwise combinations of *Clermontia*/PF *Cyanea*/OF *Cyanea*,

and/or *Galeatella*/*Trematolobelia* (*SI Appendix*, Figs. S7–S10). Given the topologies of our gene trees, it seems unlikely that interspecific gene flow could explain the divergent placement of *Cl. pyrularia*.

While HyDe does not allow us to test this directly, large blocks of significant triplets (*SI Appendix*, Figs. S9–S10) suggest that the ancestors of groups of terminals, rather than single terminals, were involved in interspecific gene flow events, although this does not discount recurrent gene flow in the history of a lineage. Deeper cases of historical gene flow may include the backbones of *Clermontia* (618 triplets, $\overline{\gamma}$ = 0.11 ± 0.13), OF *Cyanea* (1,776 triplets, $\overline{\gamma}$ = 0.26 ± 0.14), or PF *Cyanea* (318 triplets, $\overline{\gamma}$ = 0.12 ± 0.08). Ancient gene flow could explain the low nuclear backbone support and clear cytonuclear discordance in these clades, reinforced by the fact that only 51% of significant triplets involve terminals where the hybrid and donor lineages can be found on the same island today. Taken together, nuclear and plastid data suggest a pattern of introgression within, rather than among islands, with a combination of deeper introgression events as clades diversified within islands (30, 31) and more recent gene flow (30), although gene flow among islands may occur in other systems, including incipient, easily dispersed, and landscape-dominant species (28). Widespread gene flow among species of *Clermontia* on Hawai'i is in line with morphological data (6, 42), their recent divergence, and earlier analyses of cytonuclear conflict (11). While hybrids in *Cyanea* have been rarely reported, they have been noted for some species of OF *Cyanea* on Maui Nui (43). Future detailed study of gene flow within these clades is warranted, especially since hybridization may have provided additional genetic variation to drive extensive adaptive radiation and speciation in *Clermontia* and *Cyanea*—the largest and most ecologically diverse clades within the Hawaiian lobeliads—as has been suggested for a number of other highly diverse and disparate groups (44–47). For now, hybridization at the base of *Cyanea* and/or *Clermontia* appears unlikely. We note, however, that whole-genome duplication did precede the massive diversification and adaptive radiations of woody lobeliads across Africa and the Pacific Islands, paralleling a pattern seen in many angiosperm lineages (48, 49).

Convincing Evidence for the Progression Rule. Our estimated crown age of Hawaiian lobeliads of 9.88 Ma (nuclear data) or 11.61 Ma (plastid data) is generally in line with previous estimates based on different molecular datasets and dating methods (1, 2, 37). The crown age based on nuclear data is on the younger side of prior estimates, but both datasets have an overlapping 95% HPD in the 10.40 to 11.26 Ma range. The Hawaiian lobeliads—including *Sclerotheca* based on nuclear data—are the oldest and most diverse Hawaiian plant lineage known (1, 50, 51). Given an age of Ni'ihau of ~6.1 Ma (18, 19) the common ancestor of the Hawaiian lobeliads must have arrived on an older island along the Hawaiian-Emperor seamount chain and dispersed in mostly stepwise fashion to the present-day Hawaiian Islands as they emerged (1). The long stem lineages of all extant Hawaiian clades point to a long history of extinction. Predominant single-island endemism suggests that most species went extinct as island subsidence occurred. Moreover, the current clades on Kaua'i are much younger than the origin or even the end of the island's growth phase and, as with Hawaiian silverswords, may have been driven by geographic isolation as the island eroded and ridges and valleys formed (52). Similarly, peak lineage accumulation of extant clades on O'ahu also occurred well after island emergence and during the prolonged growth phase and sequential formation of parallel mountain ranges resulting from the long lag time between the activity of the Wai'anae and Ko'olau volcanoes (19), suggesting that speciation occurred as ecomorphological space or isolated landmass formed.

Many but not all previous studies of Hawaiian lineages support the progression rule (8, 20, 21, 23, 52–54). Our comprehensive sampling of the largest Hawaiian plant lineage by islands and species gives us the ability to capture repeated dispersal events. Furthermore, by breaking down widespread species into their constituent island lineages, we can more finely elucidate the pattern of interisland dispersal. Indeed, 89% of dispersal events follow the strict progression rule, with species dispersing to the next youngest, unoccupied island in the chain, with only 3% of dispersal events "jumping" adjacent islands to even younger islands. Presumably, these patterns reflect both ecological opportunity (nearby islands with few competitors) and limited dispersal (limiting movement mostly to the nearest, ecologically open islands). The progression rule is rarely violated, with movement limited to older adjacent islands, which may reflect rapid saturation of niche space within an island by closely related competitors (i.e., other lobeliads) and limited dispersal.

Most cytonuclear discordance occurs within rather than between islands. Interestingly, plastid data imply 16% more dispersal events than nuclear data. Organellar capture leading to clade homogenization appears to have occurred in PF *Cyanea* on Kaua'i (three nuclear and one plastid clade) and *Clermontia* on Hawai'i (five nuclear and two plastid clades), underestimating the number of dispersal events and ancestral range reconstructions. However, unsampled or extinct plastid lineages might also result in overestimates of dispersal events (e.g., in *Revolutella*). Given the overall pattern of discordance within, rather than between islands, the impact of gene flow on our biogeographical reconstruction is limited. Nevertheless, our findings raise the question of whether plastid phylogenies of Hawaiian plant lineages systematically overestimate the number of interisland dispersal events.

Parallel Adaptive Radiations within Islands. The process of ecological speciation in the Hawaiian lobeliads—captured in our proxies for isolation by elevation and pollinators—is mirrored by adaptive radiation within islands, a process analogous to the adaptive radiations in other dispersal-limited island or archipelago-like systems (55–59). We examined convergence in the area of a continuous ecomorphospace occupied rather than the presence of different discrete types (as in Australian marsupials, African rift-lake cichlids, and Caribbean *Anolis*, among others). In our case, *Brighamia*, *Lobelia*, and *Trematolobelia* exhibit limited disparification in elevation and flower tube length, but *Clermontia* and *Cyanea* occupy nearly the entire ecomorphological range of the Hawaiian lobeliads on these two axes, especially on Maui Nui and Hawai'i (Fig. 3). Moreover, *Cyanea* assemblages on each major island occupy roughly similar amounts of ecomorphological space, averaging 50.5% of the total available (*SI Appendix*, Fig. S17). Reduced ecomorphological disparity on Kaua'i and O'ahu is partly due to those older, more eroded/subsided islands without some higher elevations occupied by *Cyanea* on younger, taller islands (*SI Appendix*, Fig. S17) or, as in *Cyanea* species on Kaua'i, constraint due to the evolutionary history of their principal pollinators (15). Early-evolving, mostly short-billed honeycreepers may have coevolved with *Cyanea* on Kaua'i, with longer-billed species evolving later. The Hawaiian honeyeaters, another group of pollinators, arrived in the Hawaiian chain long before Kaua'i arose, but never evolved the extraordinarily long bills seen in some honeycreepers (14). Constrained by these contingencies, adaptive radiation in elevation and flower length in *Cyanea* appears to have occurred in a nearly parallel fashion on the four major islands. They did so relatively quickly, occupying nearly the same extent

of ecomorphospace on Hawai'i as on Maui Nui in just 1.2 Ma. Disparification in *Clermontia* and *Cyanea* is usually lower than expected by chance (*SI Appendix*, Figs. S19–S24), suggesting that some island radiations are constrained by the phylogenetic history of the successful colonizers.

Given that most *Cyanea*/*Clermontia* species are restricted to single islands, parallel radiations on four major islands in *Cyanea* [involving 23, 17, 32, and 12 species, respectively (*SI Appendix*, Table S2)] and on essentially two islands in *Clermontia* (involving 12 and 11 species on Maui Nui and Hawai'i) account for ~3 × 21.0 = 63 additional species of *Cyanea* and an additional 1 × 11.5 = 11.5 species of *Clermontia*, for a total of 52% of all Hawaiian lobeliad species. Radiation in flower length × elevation in these clades within islands accounts for ~21 + 11.5 = 32.5 species per island, or 22.7% of all species. The total effect of parallel radiations and single-island endemism in *Cyanea*/*Clermontia* is thus close to the total effect of within-island speciation, which accounts for 79% of all cladogenetic events (see above).

These subparallel radiations were each seeded by multiple species. Stochastic mapping indicates an average of 2.87 founding ancestral species on each island after Kaua'i for PF *Cyanea*, and 2.43 for OF *Cyanea*, for a total of 5.3 *Cyanea* founders per island. The resulting assemblages differ from the usual concept of adaptive radiation from single founders and are, in essence, "diffuse" or "interwoven" from radiations of multiple, closely related founders—and yet result in parallel patterns of community assembly. Our ability to investigate species packing in two-dimensional elevation × flower length space in these assemblages hinge on a technique that scales flower length so that it has the same effect of species turnover as a given amount of elevation. This approach should prove useful in studying species packing in two or more trait or resource dimensions in other lineages and communities.

Multiple colonists seeding the radiations of PF *Cyanea*, OF *Cyanea*, and *Clermontia* (2.52) made their survival and propagation down the Hawaiian chain over the last 7.5 to 8.0 Ma much more likely. If we model dispersal of each clade down the chain as a branching process based on a strict progression rule and a Poisson distribution of colonists, we can calculate the probabilities of lineage extinction after the appearance of one to six islands—roughly the number since *Cyanea*/*Clermontia* originated. For *Clermontia*, the probabilities of extinction on each island are 0.080, 0.074, 0.068, 0.063, 0.058, and 0.053, respectively, for a total probability of extinction of 0.396. The corresponding probabilities for PF and OF *Cyanea* are 0.296 and 0.425. In contrast, a lineage with an average of one colonist per island would have a 93.6% chance of extinction after six islands. Multiple founders forestall lineage extinction and can thereby shape adaptive radiation and species diversification.

Variation among Parallel Radiations. Hawai'i has fewer *Cyanea* species than expected based on island area and elevation, consistent with its recent emergence and incomplete colonization and in situ speciation (1). The peak in *Cyanea* diversity on Maui versus older islands is due to its greater range of habitable elevations, based on the fit to an equilibrium model explaining species number in terms of island elevation and age (1). Several other Hawaiian clades show a similar peak in diversity on Maui Nui, which has been ascribed to a shifting equilibrium involving time and island area (19), although this does not consider island elevational range, a key component of niche space. Peaks in species number per area on islands of intermediate age may be due to nonequilibrium trajectories of speciation and extinction (60, 61). However, this does not account for variation in island area and elevation. Furthermore, the power-law relationship of species number to island area ($S = kA^z$, with $z \approx 0.25$) implies that species number per area should decline with island area ($S/A \approx kA^{-0.75}$), which could create an artifactual decline in their S/A index toward the youngest and largest island. Validation of a nonequilibrium explanation for interisland variation in species richness would require eliminating this artifact and including island area and elevation in statistical analyses. This is especially true given that equilibrium views are strongly supported by static distributions (1, 19), recensuses (62), community assembly in ecomorphospace (this paper), and reconstructions of speciation rates (63, 64) in several plant and animal radiations.

Overall, diversification within the Hawaiian lobeliads appears driven by initial, rapid radiation in habitat and life-form among genera and sections of lobeliads; by nested, nearly parallel adaptive radiation and ecological speciation based on elevation and flower tube length within *Clermontia*/*Cyanea*; and by frequent interisland dispersal with widespread single-island endemism. Despite potential constraints, relatively distantly related species have diversified to occupy complementary parts of ecomorphological space, demonstrating that parallel within-island radiations by elevation and flower tube length are the result of both trait divergence within islands and convergence among islands. The observed pattern of early habitat disparification driven by ecological opportunity is in line with the predicted initial behavior of an adaptive radiation (65–67).

Relatively low variability in ecomorphospace within island assemblages indicates that, rather than populating new areas of niche space, cladogenesis within islands populates intermediate areas of niche space (*SI Appendix*, Figs. S23–S25). Indeed, filling of intermediate areas of niche space by relatively distantly related species, rather than trait conservatism, means that our parallel radiations do not fit the traditional "early burst" model of rapid initial diversification followed by stasis—a deviation that characterizes many adaptive radiations (66).

For congeners with similar niches and geographic ranges, genetic incompatibilities accumulated over time since divergence may provide additional mating barriers. Consistent with the idea that increasing genetic isolation over time can permit coexistence of closely related species, recently diverged species can be geographically isolated during initial speciation but overlap increasingly in range over the first million years after speciation (68). The possibility that other traits (e.g., flowering time) allow species with similar elevational distributions and flower tube lengths to coexist should be investigated. The nuclear and cytonuclear discordance documented herein indicates that reproductive barriers are somewhat leaky and nonsister species found in similar areas of ecomorphospace can interbreed (e.g., *Cy. lobata* subsp. *lobata*/*Cy. magnicalyx* on Maui and *Cl. clermontioides*/*Cl. montis-loa* on Hawai'i). In *Cyanea*, some closely related species that occupy similar parts of ecomorphospace on the same island might reflect allopatric speciation on different parts of that island facilitated by limited seed-dispersal distances, associated with relatively sedentary frugivorous birds of forest interiors (1, 8, 56).

Coda. This study represents the largest phylogenomic analysis of any Hawaiian lineage in terms of total species sampled. As such, we were able not only to address sources of phylogenomic discordance across the radiation, but also date and infer repeated patterns of dispersal, isolation, parallel adaptive radiation on different islands, and allopatric speciation within and among islands. Our well-resolved phylogeny greatly extends previous findings of a progression rule in studies of a few species of *Cyanea* (7, 8) to a dense sampling of the Hawaiian lobeliad clade (including *Sclerotheca*).

The initial rapid divergence by habitat in the Hawaiian lobeliads accords with the expected pattern of trait disparification in adaptive radiations, in which niche breadth is filled early in diversification (but see refs. 66 and 69). Subsequent parallel adaptive radiations driven by ecological speciation within each major island—a major finding of this paper supporting an earlier hypothesis (1)—results in nonsister species occupying nearby parts of niche space. Any breakdown of extrinsic barriers to reproduction most likely occurs at the beginning of radiations within islands as species and ecomorphological traits initially diverge as well as later when subsequent ecological speciation places more distantly related species in neighboring niche spaces within an island. Given the expected effects of moderate dispersal ability, competition, and selection for adaptive radiation and mating barriers (1, 51, 55–65), especially in rapidly speciating, ecologically dominant groups where competition among close relatives is likely to be more important than competition with others in driving divergence (56), similar patterns of parallel adaptive radiations and historical gene flow should emerge as the number of phylogenomic investigations of Hawaiian plant lineages continues to grow.

Materials and Methods

DNA Samples. We included 101 of the 114 extant species of Hawaiian lobeliads, represented by 188 ingroup samples, plus eight outgroups (*SI Appendix*, Table S10). Our aim was to include one accession for each extant species and subspecies from each volcano on which it occurs. Total genomic DNAs were used from earlier studies or represented new collections. For new collections, leaf tissue was stored on silica gel prior to DNA extraction using DNeasy Plant Mini Kits (Qiagen, Valencia, CA) following the manufacturers protocol.

Nuclear Data. We targeted ~500 exons identified in an across-angiosperm analysis of single-copy nuclear loci (70, 71). To improve enrichment efficiency and extent of sequence variation captured, we targeted flanking regions that aligned well across Hawaiian lobeliads using low coverage sequencing of entire genomes (~15×) of *Cl. lindseyana* and *Cy. pilosa*. Following sequencing, we demultiplexed reads passing the Casava *highchastity* filter in the Illumina software, with no index mismatches tolerated. We then merged overlapping read pairs following (72) to remove library adapters and correct sequencing errors. Using established pipelines (73, 74), we used a quasi-de novo approach to generate aligned assemblies for 389 putatively orthologous loci.

Hawaiian lobeliads segregate as diploid (75), but there were a high number of ambiguous base calls in our initial alignments of putative orthologs. Given the ancient whole genome duplication within Lobelioideae ~15 to 20 Ma (75–78), associated with acquisition of the woody habit in the ancestor of the Pacific Island, African, and Asian lobeliads, this raised concerns that our initial assembly contained paralogs. We therefore remapped all demultiplexed reads to the majority-rule consensus sequence of each locus using HybPiper v.2.1.3 (79), mapping with the *bwa* algorithm (80), with potential homolog sequences needing to ≥50% of the length of the reference to be included. Potential paralogs were extracted using the script "paralog_retriver.py," with 386 reassembled loci possessing a manageable number of potential paralogs. For each group of homologs, potential nonchimeric paralogs were aligned in MAFFT v.7.490 (81) using the function *mafft* in ips v.0.0.11 (82). Maximum likelihood gene trees for each group of homologs were generated using the function *optim.pml* under the GTR model followed by 100 bootstrap (BS) replicates using the function *bootstrap.pml* in phangorn v.2.11.1 (83). Orthologs in each homolog cluster were sorted using OrthoSNAP (84), collapsing branches with BS < 80 and only retaining ortholog clusters with >40 terminals. OrthoSNAP returned 691 ortholog clusters, 62 of which were single copy, for a mean = 1.79 ± 0.62 SD orthologs per homolog. Orthologs were realigned using MAFFT and visually inspected. Poor alignments were discarded, questionable sequences were trimmed or completely removed from alignments as necessary, and samples with poor locus recovery removed entirely, resulting in a final dataset of 179 terminals, 633 loci (mean = 153.5 ± 26.5 samples/locus, 14% missing sequences overall), and 1,139,014 aligned nucleotides (mean = 1,799.4 ± 764.4 SD nucleotides/locus).

Plastomes. We generated both exon-only and complete plastome alignments. We assembled exons by first annotating a reference sequence of *Cl. fauriei* using Chloë (85). We extracted each annotated region, discarding rRNA, tRNA, and second inverted repeat regions, with the 76 resulting exons used as references to assemble raw reads in HybPiper.

To assemble complete plastomes, we employed a reference-guided de novo assembly using GetOrganelle v.1.7.7.0 (86). We tested various combinations of parameters, with final parameters -R 20 -k 21,35,45,65,75,85,105,127. The seed sequence for each sample was selected based on the closest relative with a reference plastome available on GenBank (*SI Appendix*, Table S11). Consensus sequences were generated by mapping assembled contigs back onto the appropriate reference plastome in Geneious (87). Regions with a high mismatch score from the reference were trimmed manually. We expanded outgroup sampling by adding 22 plastomes from GenBank (*SI Appendix*, Table S11). Datasets were aligned using MAFFT, with alignments automatically trimmed using TrimAL v.1.4 (88) and further inspected manually. Samples with ≥50% missing data were excluded from further analysis.

Phylogenetic Analyses. We selected the best nucleotide substitution model for each nuclear locus using IQ-TREE v.2.2.2.6 (89). Then, we reconstructed a phylogenetic tree for the concatenated, partitioned, nuclear data under the optimal substitution model for each locus using IQ-TREE with 1,000 ultrafast bootstrap replicates using the GENESTE resampling of partitions and then sites within resampled partitions. Plastome genealogies were inferred in the same way using the exon-only dataset, but for the complete plastome we assumed a single partition under GTR+I+Γ.

Next, to examine how assuming a model consistent with the multispecies coalescent might affect the nuclear topology, we used weighted ASTRAL in ASTER v.1.15.2.3 (90, 91). We provided ASTRAL with gene trees for each locus inferred using IQ-TREE as above, with ASTRAL searches consisting of 16 search rounds with 16 rounds of subsampling each round. To visualize conflict among nuclear topologies, bootstrap replicates from the IQ-TREE analysis were mapped onto the ASTRAL topology using SumTrees in DendroPy v.4.6.1 (92).

Addressing Deep Discordance. Potential deep nuclear and cytonuclear discordance among the major clades of Hawaiian lobeliads plus *Sclerotheca* was explored in three ways. First, gene tree support for possible clades within our inferred gene trees was visualized using DiscoVista (93). We examined gene tree support for both the major clades in our ASTRAL population tree, as well as support for alternative backbone clades.

Second, to address possible deep reticulate evolution, we used PhyloNetworks v.0.15.3 (94, 95) to estimate semidirected phylogenetic networks. For each gene tree, we randomly selected one placeholder terminal from each of the eight genera/sections (one placeholder for each clade of *Cyanea*), plus one outgroup. We only used loci containing all 10 terminals (n = 471) and generated 10 such placeholder datasets. For each placeholder dataset, we first generated concordance factors from the set of gene trees using the function *readTrees2CF*. Then, we estimated phylogenetic networks using the *snaq!* function; testing hypotheses of up to 0, 1, or 2 reticulations (h) per set of trees, with 10 search replicates per value of h and identical starting seeds. The backbone ASTRAL topology was used as a starting tree for searches where h = 0, otherwise the best topology from the h-1 search was used. Models were compared using their pseudolikelihood score (95). Based on our sampling strategy, any differences among best networks should be due to phylogenetic uncertainty. To summarize all 10 networks, we constructed the majority-rule consensus tree using each major topology from the best-fitting network for each placeholder dataset, manually adding the hybridization signal most frequent among the 10 networks.

Third, we addressed cytonuclear discordance by testing the hypothesis that clades observed in the plastome tree but not the nuclear tree could be explained by ILS alone. Using the ASTRAL tree, we simulated 5,000 nuclear gene trees using the function *sim.coal.mpest* in Phybase v.2.0 (96). Then, simulated trees were summarized onto the constrained exon-only plastid tree as a measure of bipartition support for plastid clades under the expected distribution of nuclear gene trees using SumTrees. Finally, we scored the plastid tree using the simulated nuclear trees as input using ASTRAL v.5.7.8.

Interspecific Gene Flow. Given its size, our entire dataset was not tractable for inferring explicit phylogenetic networks. We therefore screened for interspecific gene flow through assessing site pattern probabilities. We analyzed the concatenated nuclear alignment using HyDe v.0.4.3 (97). To reduce the number of rooted quartets, we provided a mapping file guided by well-supported infraspecific clades recovered in our ASTRAL tree, containing 107 ingroup terminals (595,455 quartets).

Divergence Time Estimation. Due to the large size of the dataset in both number of individuals and loci, we selected representative loci to calibrate trees to absolute time. For the nuclear data, we used the ASTRAL tree with all branches with LPP < 0.90 collapsed to guide locus selection. We collapsed branches in each gene tree with BS < 33 and calculated the Robinson–Foulds similarity of each collapsed gene tree to the collapsed ASTRAL topology using the R package "TreeDist" v.2.0.3 (98). To minimize missing data, we filtered alignments based on a combination of containing the ultimate outgroup of *L. nubigena*, median BS > 50, and sample coverage ≥170, retaining the 13 loci most similar to the ASTRAL topology and further removing samples with low coverage across the selected loci for a total of 163 terminals and 23,129 aligned bp. Dropped individuals were all species with multiple samples that fell sister to conspecific samples in the full dataset. We calibrated the nuclear tree using BEAST2 v.2.7.5 (99) with a single partition and the GTR+I+Γ model with branch rates estimated under the optimized relaxed clock (100) and birth–death tree prior. The posterior distribution of trees was constrained to contain nodes of the ASTRAL topology with LPP > 0.9. We applied 11 age priors based on two secondary dates (37) and nine priors based on the geologic ages of Hawai'i, Marquesas, Maui Nui, or O'ahu (refs. 19 and 101 and *SI Appendix*, Table S12). We used a uniformly distributed prior on secondary dates, with the minimum and maximum ages corresponding to the 95% HPD of estimated node ages and a normally distributed prior on island ages. Mean island age was based on the mean age for island habitability, with the SD of each prior was set such that the upper bound of the 95% quantile for the prior matched the minimum and maximum estimated ages of island habitability. We ran each analysis for 100 million generations, with trees and parameters logged every 10,000 generations. Following a 25% burn-in, the posterior distribution of trees was summarized using TreeAnnotator by calculating both the maximum clade credibility tree and by summarizing on the ASTRAL topology and calculating common ancestor node heights.

For the plastome tree, we assumed that the genealogy based on data from exons and spacers was a better estimate of relationships than the genealogy based on exons alone. However, because fewer samples were present in the alignment containing exons and spacers, we first used the ML topology from that dataset to constrain the exon-only tree, collapsing branches of the constraint topology with BS < 75, estimated in IQ-TREE as described above. Next, we selected the exons present for >200/212 terminals, >800 bp in length, and with > 5% of sites being parsimony informative, resulting in a dataset of 200 terminals and 14 exons for a total length of 24,371 aligned bp. BEAST parameters, chain lengths, testing alternative tree priors, and tree summarization were the same as for the nuclear data except for the following modifications. First, we estimated site models for each exon using the best nucleotide substitution model selected in IQ-TREE, keeping clock and tree models linked. Second, we fixed the topology to match that of the supported (BS > 75) nodes of the constrained exon-only ML tree. Third, the expanded outgroup sampling in the plastid dataset allowed us to add an additional secondary date prior. Last, because the nuclear clade of OF *Cyanea* on Maui Nui was not monophyletic, we split the prior into two constraints.

Historical Biogeography. Since initial results indicated that species may not be monophyletic and we were also interested in understanding infraspecific patterns of dispersal, we scored species/subspecies × island combination for one of four island groups: Kaua'i (including Ni'ihau), O'ahu, Maui Nui (Lāna'i, Maui, and Moloka'i), or Hawai'i, or two extra-Hawaiian areas: Africa/Asia and Polynesia. Scoring was based on the provenance of the sample, apart from three cases where a multi-island species/subspecies were only represented by a single terminal, in which case the tip was scored for the full range of the taxon. Under the coding scheme of four-island groups, our sampling contained 109/159 possible island × species combinations (87% of extant combinations).

We estimated ancestral areas on each BEAST chronogram using the maximum-likelihood approach implemented in BioGeoBEARS v.1.1.3 (102, 103). We allowed each range to contain up to two areas and conducted a stratified analysis, disallowing dispersal to Hawaii prior to the maximum estimated age of island habitability. Because the Hawaiian lobeliads are much older than the maximum age of Kaua'i, we did not use the age of that island to restrict dispersal. Thus, "Kaua'i" effectively becomes "Kaua'i or older." We employed a dispersal multiplier to modify the dispersal probability among areas: 0.75 for dispersal to adjacent Hawaiian Islands, 0.25 for dispersal within Hawaii but to nonadjacent Hawaiian Islands, or 0.1 for dispersal among areas outside the Hawaiian Islands. We compared model fit between DEC (dispersal-extinction-cladogenesis; ref. 104) and DEC+J. For each model, we generated 100 stochastic maps to tally the average number of interisland dispersal events between each pair of islands to examine how many conformed to the progression rule.

Ecological Diversification among and within Islands. To further explore patterns of diversification within and across island groups, we gathered trait data for elevation and flower length as proxies for divergence in habitat and pollination system, respectively. We took the midpoint of reported range of each trait, keeping each island a separate data point for multi-island species. Elevational information was supplemented by GBIF data (https://www.gbif.org/), and the mean from these data superseded reported ranges, when available. GBIF names were standardized based on our list of accepted taxa (*SI Appendix*, Table S1). The entire process of cleaning GBIF records is fully documented and reproducible in the code available in the Dryad repository accompanying this paper (105).

We reconstructed the ecomorphospace of Hawaiian lobeliads as a biplot of mean elevation and midpoint flower length and overlaid the nuclear chronogram to generate a phyloecomorphospace that connects species based on their known relationships. After excluding *Brighamia*, which is a clear outlier in both elevation and flower length, associated with low-elevation sea cliffs and hawkmoth pollination (unique in a clade otherwise marked by bird pollination), we examined the partitioning of ecomorphospace among islands, clades, and islands × clades. To place both variables on similar scales, we calculated the ratio of the ranges of elevation and flower length (maximum maxima minus minimum minima across all species). This yielded a ratio of 27.92 for all species and 28.31 for both *Cyanea* and *Clermontia*/*Cyanea*. We multiplied flower lengths by the appropriate factor for the focal clade in each analysis.

Following standardization, we visualized the two-dimensional clustering of the breadth of ecomorphospace among clades and clades × islands as biplots of both traits. We further investigated the scatter by calculating the convex hull hypervolume for each grouping using the *chull* function (106). Because they comprise the vast majority of species diversity in Hawaiian lobeliads, we broke out *Clermontia* and *Cyanea* (the latter both binned as an ecological grouping and treated as two clades) to further examine trait disparification. Using the function *dispRity.per.group* in dispRity v.1.6.8 (107), we both quantified the breadth of ecomorphospace occupied by each clade × island combination as a convex hull hypervolume and examined differentiation among species within each grouping calculated as the sum of variances in each variable. Differences between groupings were tested using 100 rarefied bootstrap pseudoreplicates with the *test.dispRity* function. Hypothesis tests consisted of Wilcoxon rank sum tests on the bootstrap pseudoreplicates of each combination containing >four species, with a Bonferroni correction for multiple comparisons. Under a scenario of ecological speciation within islands, we expect the extent of ecomorphological space occupied to increase with species number. We also expect high variance among congeners.

For each island × clade combination, we also examined how disparity varies compared to that expected under a random assemblage of species by testing the observed value of each disparity metric described above against values generated from 100 random, equally sized assemblages of congeners. The significance of the observed value of each metric compared to that of random assemblages was assessed using a one-sample *t*-test. Under a scenario of ecological speciation, we expect observed assemblages to vary the same or more than a random sample of species.

Data, Materials, and Software Availability. Raw reads have been deposited in the NCBI Sequence Read Archive under BioProject PRJNA1217876 (108). Nucleotide alignments, phylogenetic trees, trait data, and code data have been deposited in Dryad (Dryad: https://doi.org/10.5061/dryad.zpc866tj1) (105).

ACKNOWLEDGMENTS. This work is an extension of the PhD thesis of Steven J. Hunter, who spent many hours in the field and lab collecting and preparing the samples used in this study. Thanks to N. Agorastos, R. Akau, J. Kualiʻi Camara, S. Crysdale, J. Johansen, Z. Judd, R. Loo, S. McDaniel, L. Perry, J. VanDeMark, H. Oppenheimer, A. Bakutis, S. Ching-Harbin, L. Weisenberger, W. Kishida, N. Tangalin, M. Edmonds, D. Lorence, and S. Perlman, for assistance with collecting specimens and fieldwork, C. Dang and A. Marshall for help with permitting, and T. Sakishima and D. Spalink for assistance in DNA extraction. We are also grateful to M. Kortyna at Florida State University's Center for Anchored Phylogenomics for assistance with data collection. This work was made possible through grants from the NSF (DGE-1256259, DEB-1702007, DEB-1929296), the Graduate School of the University of Wisconsin-Madison, and the Office of the Vice Chancellor for Research and Graduate Education at the University of Wisconsin-Madison with funding from the Wisconsin Alumni Research Foundation.

Author affiliations: [a]Department of Botany, University of Wisconsin-Madison, Madison, WI 53706; [b]Department of Land and Natural Resources, Division of Forestry and Wildlife, Lihue, HI 96766; [c]School of Life Sciences, University of Nevada-Las Vegas, Las Vegas, NV 89154; [d]National Tropical Botanical Garden, Kalāheo, HI 96756; [e]Department of Biological Science, Florida State University, Tallahassee, FL 32306; [f]Department of Scientific Computing, Florida State University, Tallahassee, FL 32306; and [g]Department of Statistics, University of Wisconsin-Madison, Madison, WI 53706

1. T. J. Givnish *et al.*, Origin, adaptive radiation and diversification of the Hawaiian lobeliads (Asterales: Campanulaceae). *Proc. Biol. Sci.* **276**, 407–416 (2009).
2. E. B. Knox, C. Li, The East Asian origin of the giant lobelias. *Am. J. Bot.* **104**, 924–938 (2017).
3. W. L. Wagner, D. R. Herbst, S. H. Sohmer, *Manual of the Flowering Plants of Hawai'i* (University of Hawai'i and Bishop Museum Press, Honolulu, HI, ed. 2, 1999), vols. 1 and 2.
4. W. L. Wagner, D. R. Herbst, D. H. Lorence, Flora of the Hawaiian Islands. http://botany.si.edu/pacificislandbiodiversity/hawaiianflora/index.html. Accessed 17 July 2024.
5. S. Carlquist, *Island Life* (American Museum of Natural History, New York, NY, 1965).
6. S. Carlquist, *Hawaii: A Natural History* (National Tropical Botanical Garden, Lawai, HI, 1992).
7. T. J. Givnish, K. J. Sytsma, J. F. Smith, W. J. Hahn, Thorn-like prickles and heterophylly in *Cyanea*: Adaptations to extinct avian browsers on Hawaii? *Proc. Natl. Acad. Sci. U.S.A.* **91**, 2810–2814 (1994).
8. T. J. Givnish, K. J. Sytsma, J. F. Smith, W. J. Hahn, "Molecular evolution, adaptive radiation, and geographic speciation in *Cyanea* (Campanulaceae, Lobelioideae)" in *Hawaiian Biogeography: Evolution on a Hot Spot Archipelago*, W. L. Wagner, V. Funk, Eds. (Smithsonian Institution Press, Washington, D.C., 1995), pp. 288–337.
9. T. J. Givnish, "Adaptive radiation, dispersal, and diversification of the Hawaiian lobeliads" in *The Biology of Biodiversity*, M. Kato, Ed. (Springer-Verlag, Tokyo, 1999), pp. 67–90.
10. T. J. Givnish, R. A. Montgomery, G. Goldstein, Adaptive radiation of photosynthetic physiology in the Hawaiian lobeliads: Light regimes, static light responses, and whole-plant compensation points. *Am. J. Bot.* **91**, 228–246 (2004).
11. T. J. Givnish, G. J. Bean, M. Ames, S. P. Lyon, K. J. Sytsma, Phylogeny, floral evolution, and inter-island dispersal in Hawaiian *Clermontia* (Campanulaceae) based on ISSR variation and plastid spacer sequences. *PLoS One* **8**, e62566 (2013).
12. R. A. Montgomery, T. J. Givnish, Adaptive radiation of photosynthetic physiology in the Hawaiian lobeliads: Dynamic photosynthetic responses. *Oecologia* **155**, 455–467 (2008).
13. C. Scoffoni *et al.*, Light-induced plasticity in leaf hydraulics, venation, anatomy, and gas exchange in ecologically diverse Hawaiian lobeliads. *New Phytol.* **207**, 43–58 (2015).
14. R. C. Fleischer, H. F. James, S. L. Olson, Convergent evolution of Hawaiian and Australo-Pacific honeyeaters from distant songbird ancestors. *Curr. Biol.* **18**, 1927–1931 (2008).
15. H. R. Lerner, M. Meyer, H. F. James, M. Hofreiter, R. C. Fleischer, Multilocus resolution of phylogeny and timescale in the extant adaptive radiation of Hawaiian honeycreepers. *Curr. Biol.* **21**, 1838–1844 (2011).
16. M. P. Kambysellis, E. M. Craddock, "Ecological and reproductive shifts in the diversification of the endemic Hawaiian Drosophila" in *Molecular Evolution and Adaptive Radiation*, T. J. Givnish, K. J. Sytsma, Eds. (Cambridge University Press, New York NY, 1997), pp. 475–509.
17. P. M. O'Grady *et al.*, Phylogenetic and ecological relationships of the Hawaiian Drosophila inferred by mitochondrial DNA analysis. *Mol. Phylogenet. Evol.* **58**, 244–256 (2011).
18. D. A. Clague, D. R. Sherrod, "Growth and degradation of Hawaiian volcanoes" in *Characteristics of Hawaiian Volcanoes*, M. P. Poland, T. J. Takahashi, C. M. Landowski, Eds. (US Geological Survey No. 1801-3, Reston, VA, 2014), pp. 97–146.
19. J. Y. Lim, C. R. Marshall, The true tempo of evolutionary radiation and decline revealed on the Hawaiian archipelago. *Nature* **543**, 710–713 (2017).
20. V. A. Funk, W. L. Wagner, "Biogeography of seven ancient Hawaiian plant lineages" in *Hawaiian Biogeography: Evolution on a Hotspot Archipelago*, W. L. Wagner, V. A. Funk, Eds. (Smithsonian Institution Press, Washington D.C., 1995), pp. 160–194.
21. K. L. Shaw, R. G. Gillespie, Comparative phylogeography of oceanic archipelagos: Hotspots for inferences of evolutionary process. *Proc. Natl. Acad. Sci. U.S.A.* **113**, 7986–7993 (2016).
22. B. G. Baldwin, K. R. Wood, W. A. Freyman, Directionally biased habitat shifts and biogeographically informative cytonuclear discordance in the Hawaiian silversword alliance (Compositae). *Am. J. Bot.* **108**, 2015–2037 (2021).
23. R. H. Cowie, B. S. Holland, Molecular biogeography and diversification of the endemic terrestrial fauna of the Hawaiian Islands. *Proc. Biol. Sci.* **363**, 3363–3376 (2008).
24. M. S. Appelhans, C. Paetzold, K. R. Wood, W. L. Wagner, RADseq resolves the phylogeny of Hawaiian *Myrsine* (Primulaceae) and provides evidence for hybridization. *J. Syst. Evol.* **58**, 823–840 (2020).
25. M. L. Knope, M. R. Bellinger, E. M. Datlof, T. J. Gallaher, M. A. Johnson, Insights into the evolutionary history of the Hawaiian *Bidens* (Asteraceae) adaptive radiation revealed through phylogenomics. *J. Hered.* **111**, 119–137 (2020).
26. M. A. Johnson, Y. Pillon, T. Sakishima, D. K. Price, E. A. Stacy, Multiple colonizations, hybridization and uneven diversification in *Cyrtandra* (Gesneriaceae) lineages on Hawai'i Island. *J. Biogeogr.* **46**, 1178–1196 (2019).
27. K. N. Magnacca, D. K. Price, Rapid adaptive radiation and host plant conservation in the Hawaiian picture wing *Drosophila* (Diptera: Drosophilidae). *Mol. Phylogenet. Evol.* **92**, 226–242 (2015).
28. J. Y. Choi *et al.*, Ancestral polymorphisms shape the adaptive radiation of *Metrosideros* across the Hawaiian Islands. *Proc. Natl. Acad. Sci. U.S.A.* **118**, e2023801118 (2021).
29. J. R. Dupuis *et al.*, Targeted amplicon sequencing of 40 nuclear genes supports a single introduction and rapid radiation of Hawaiian *Metrosideros* (Myrtaceae). *Plant Syst. Evol.* **305**, 961–974 (2019).
30. J. A. Kleinkopf, W. R. Roberts, W. L. Wagner, E. H. Roalson, Diversification of Hawaiian *Cyrtandra* (Gesneriaceae) under the influence of incomplete lineage sorting and hybridization. *J. Syst. Evol.* **57**, 561–578 (2019).
31. C. Paetzold, K. R. Wood, D. A. Eaton, W. L. Wagner, M. S. Appelhans, Phylogeny of Hawaiian *Melicope* (Rutaceae): RAD-seq resolves species relationships and reveals ancient introgression. *Front. Plant Sci.* **10**, 1074 (2019).
32. C. M. Tomlin *et al.*, Allopolyploid origin and diversification of the Hawaiian endemic mints. *Nat. Commun.* **15**, 3109 (2024).
33. R. J. Pender, "Floral trait evolution and pollination ecology in the Hawaiian lobeliad genus, Clermontia *(Campanulaceae)*," PhD dissertation, University of Hawaii, Manoa, Honolulu, HI (2013), 17 June 2024.
34. S. J. Hunter, "Phylogeny and historical biogeography of the native Hawaiian lobeliads (Campanulaceae: Lobelioideae)," PhD dissertation, The University of Wisconsin-Madison, Madison, WI (2018), 17 June 2024.
35. Y. Pillon, E. Stacy, J. Y. Meyer, Phylogenetics and systematics of the South Polynesian genera *Apetahia* and *Sclerotheca* (Campanulaceae subfam. Lobelioideae). *Bot. Lett.* **165**, 186–192 (2018).
36. A. Antonelli, Have giant lobelias evolved several times independently? Life form shifts and historical biogeography of the cosmopolitan and highly diverse subfamily Lobelioideae (Campanulaceae). *BMC Biol.* **7**, 1–21 (2009).
37. L. Y. Chen, Q. F. Wang, S. S. Renner, East Asian Lobelioideae and ancient divergence of a giant rosette *Lobelia* in Himalayan Bhutan. *Taxon* **65**, 293–304 (2016).
38. C. J. Li, X. Xie, H. Liu, R. N. Wang, D. Z. Li, Plastome evolution in the East Asian lobelias (Lobelioideae) using phylogenomic and comparative analyses. *Front. Plant Sci.* **14**, 1144406 (2023).
39. J. H. Degnan, N. A. Rosenberg, Gene tree discordance, phylogenetic inference and the multispecies coalescent. *Trends Ecol. Evol.* **24**, 332–340 (2009).
40. J. H. Degnan, Anomalous unrooted gene trees. *Syst. Biol.* **62**, 574–590 (2013).
41. L. Liu, Z. Xi, C. C. Davis, Coalescent methods are robust to the simultaneous effects of long branches and incomplete lineage sorting. *Mol. Biol. Evol.* **32**, 791–805 (2015).
42. T. G. Lammers, Systematics of *Clermontia* (Campanulaceae-Lobelioideae). *Syst. Bot. Monogr.* **20**, 1–97 (1991).
43. T. G. Lammers, "Campanulaceae" in *Manual of the Flowering Plants of Hawai'i*, W. L. Wagner, D. R. Herbst, S. H. Sohmer, Eds. (University of Hawai'i and Bishop Museum Press, Honolulu, HI, ed. 2, 1999), vols. 1 and 2, pp. 420–489.
44. P. R. Grant, B. R. Grant, Phenotypic and genetic effects of hybridization in Darwin's finches. *Evolution* **48**, 297–316 (1994).
45. K. Kagawa, G. Takimoto, Hybridization can promote adaptive radiation by means of transgressive segregation. *Ecol. Lett.* **21**, 264–274 (2018).
46. J. I. Meier *et al.*, Cycles of fusion and fission enabled rapid parallel adaptive radiations in African cichlids. *Science* **381**, eade2833 (2023).
47. O. Seehausen, Hybridization and adaptive radiation. *Trends Ecol. Evol.* **19**, 198–207 (2004).
48. D. C. Tank *et al.*, Nested radiations and the pulse of angiosperm diversification: Increased diversification rates often follow whole genome duplications. *New Phytol.* **207**, 454–467 (2015).
49. N. Walden *et al.*, Nested whole-genome duplications coincide with diversification and high morphological disparity in Brassicaceae. *Nat. Commun.* **11**, 3795 (2020).
50. M. S. Appelhans, J. Wen, M. Duretto, D. Crayn, W. L. Wagner, Historical biogeography of *Melicope* (Rutaceae) and its close relatives with a special emphasis on Pacific dispersals. *J. Syst. Evol.* **56**, 576–599 (2018).
51. J. P. Price, W. L. Wagner, Speciation in Hawaiian angiosperm lineages: Cause, consequence, and mode. *Evolution* **58**, 2185–2200 (2004).
52. M. J. Landis, W. A. Freyman, B. G. Baldwin, Retracing the Hawaiian silversword radiation despite phylogenetic, biogeographic, and paleogeographic uncertainty. *Evolution* **72**, 2343–2359 (2018).
53. D. H. Hembry *et al.*, Insect radiations on islands: Biogeographic pattern and evolutionary process in Hawaiian insects. *Q. Rev. Biol.* **96**, 247–296 (2021).
54. M. Nepokroeff, K. J. Sytsma, W. L. Wagner, E. A. Zimmer, Reconstructing ancestral patterns of colonization and dispersal in the Hawaiian understory tree genus *Psychotria* (Rubiaceae): A comparison of parsimony and likelihood approaches. *Syst. Biol.* **52**, 820–838 (2003).
55. E. D. Burress *et al.*, Island-and lake-like parallel adaptive radiations replicated in rivers. *Proc. Biol. Sci.* **285**, 20171762 (2018).
56. T. J. Givnish, Ecology of plant speciation. *Taxon* **59**, 1326–1366 (2010).
57. P. R. Grant, B. R. Grant, *How and Why Species Multiply: The Radiation of Darwin's Finches* (Princeton University Press, Princeton NJ, 2007).
58. A. H. Patton *et al.*, When adaptive radiations collide: Different evolutionary trajectories between and within island and mainland lizard clades. *Proc. Natl. Acad. Sci. U.S.A.* **118**, e2024451118 (2021).
59. O. Seehausen, African cichlid fish: A model system in adaptive radiation research. *Proc. Biol. Sci.* **273**, 1987–1998 (2006).
60. R. Gillespie, Community assembly through adaptive radiation in Hawaiian spiders. *Science* **303**, 356–359 (2004).
61. R. Gillespie, B. Baldwin, "Island biogeography of remote archipelagoes: Interplay between ecological and evolutionary processes" in *The Theory of Island Biogeography Revisited*, J. B. Losos, R. E. Ricklefs, Eds. (Princeton University Press, Princeton, N.J, 2010), pp. 358–387.
62. D. S. Simberloff, E. O. Wilson, Experimental zoogeography of islands: A two-year record of colonization. *Ecology* **51**, 934–937 (1970).
63. A. B. Philimore, T. D. Price, Density dependent cladogenesis in birds. *PLoS Biol.* **6**, e71 (2008).

64. D. L. Rabosky, R. E. Glor, Equilibrium speciation dynamics in a model radiation of island lizards. *Proc. Natl. Acad. Sci. U.S.A.* **107**, 22178–22183 (2010).
65. S. Gavrilets, J. B. Losos, Adaptive radiation: Contrasting theory with data. *Science* **323**, 732–737 (2009).
66. L. J. Harmon *et al.*, Early bursts of body size and shape evolution are rare in comparative data. *Evolution* **64**, 2385–2396 (2010).
67. D. Schluter, *The Ecology of Adaptive Radiation* (Oxford University Press, Oxford, 2000).
68. N. Karimi *et al.*, Chromosomal evolution, environmental heterogeneity, and migration drive spatial patterns of species richness in *Calochortus* (Liliaceae). *Proc. Natl. Acad. Sci. U.S.A.* **121**, e2305228121 (2024).
69. J. J. Schenk, S. Jacobs, L. Hufford, Comparative diversification analyses of Hydrangeaceae and Loasaceae reveal complex evolutionary history as species disperse out of Mesoamerica. *Amer. J. Bot.* **112**, e16455 (2025).
70. C. Buddenhagen *et al.*, Anchored phylogenomics of angiosperms I: Assessing the robustness of phylogenetic estimates. BioRxiv [Preprint] (2016). https://www.biorxiv.org/content/10.1101/086298v2 (Accessed 17 June 2024).
71. D. Bogarín *et al.*, Anchored hybrid enrichment generated nuclear, plastid and mitochondrial markers resolve the *Lepanthes horrida* (Orchidaceae: Pleurothallidinae) species complex. *Mol. Phyl. Evol.* **129**, 27–47 (2018).
72. D. R. Rokyta, A. R. Lemmon, M. J. Margres, K. Aronow, The venom-gland transcriptome of the eastern diamondback rattlesnake (*Crotalus adamanteus*). *BMC Genom.* **13**, 1–23 (2012).
73. C. A. Hamilton, A. R. Lemmon, E. M. Lemmon, J. E. Bond, Expanding anchored hybrid enrichment to resolve both deep and shallow relationships within the spider tree of life. *BMC Evol. Biol.* **16**, 1–20 (2016).
74. R. O. Prum *et al.*, A comprehensive phylogeny of birds (Aves) using targeted next-generation DNA sequencing. *Nature* **526**, 569–573 (2015).
75. T. G. Lammers, Chromosome numbers and their systematic implications in Hawaiian Lobelioideae (Campanulaceae). *Am. J. Bot.* **75**, 1130–1134 (1988).
76. E. B. Knox, S. R. Downie, J. D. Palmer, Chloroplast genome rearrangements and the evolution of giant lobeliads from herbaceous ancestors. *Mol. Biol. Evol.* **10**, 414–430 (1993).
77. T. G. Lammers, Chromosome numbers of Campanulaceae. III. Review and integration of data for subfamily Lobelioideae. *Am. J. Bot.* **80**, 660–675 (1993).
78. A. A. Crowl *et al.*, A global perspective on Campanulaceae: Biogeographic, genomic, and floral evolution. *Am. J. Bot.* **103**, 233–245 (2016).
79. M. G. Johnson *et al.*, HybPiper: Extracting coding sequence and introns for phylogenetics from high-throughput sequencing reads using target enrichment. *Appl. Plant Sci.* **4**, 1600016 (2016).
80. H. Li, R. Durbin, Fast and accurate short read alignment with Burrows-Wheeler transform. *Bioinformatics* **25**, 1754–1760 (2009).
81. K. Katoh, D. M. Standley, MAFFT multiple sequence alignment software version 7: Improvements in performance and usability. *Mol. Biol. Evol.* **30**, 772–780 (2013).
82. C. Heibl, PHYLOCH: R language tree plotting tools and interfaces to diverse phylogenetic software packages. http://www.christophheibl.de/Rpackages.html. Accessed 17 June 2024.
83. K. P. Schliep, phangorn: Phylogenetic analysis in R. *Bioinformatics* **27**, 592–593 (2011).
84. J. L. Steenwyk *et al.*, OrthoSNAP: A tree splitting and pruning algorithm for retrieving single-copy orthologs from gene family trees. *PLoS Biol.* **20**, e3001827 (2022).
85. X. Zhong, "Assembly, annotation and analysis of chloroplast genomes," PhD dissertation, The University of Western Australia, Perth, Australia (2020), 17 June 2024.
86. J. J. Jin *et al.*, GetOrganelle: A fast and versatile toolkit for accurate de novo assembly of organelle genomes. *Genome Biol.* **21**, 1–31 (2020).
87. M. Kearse *et al.*, Geneious Basic: An integrated and extendable desktop software platform for the organization and analysis of sequence data. *Bioinformatics* **28**, 1647–1649 (2012).
88. S. Capella-Gutiérrez, J. M. Silla-Martínez, T. Gabaldón, trimAl: A tool for automated alignment trimming in large-scale phylogenetic analyses. *Bioinformatics* **25**, 1972–1973 (2009).
89. B. Q. Minh *et al.*, IQ-TREE 2: New models and efficient methods for phylogenetic inference in the genomic era. *Mol. Biol. Evol.* **37**, 1530–1534 (2020).
90. S. Mirarab *et al.*, ASTRAL: Genome-scale coalescent-based species tree estimation. *Bioinformatics* **30**, i541–i548 (2014).
91. C. Zhang, S. Mirarab, Weighting by gene tree uncertainty improves accuracy of quartet-based species trees. *Mol. Biol. Evol.* **39**, msac215 (2022).
92. J. Sukumaran, M. T. Holder, DendroPy: A Python library for phylogenetic computing. *Bioinformatics* **26**, 1569–1571 (2010).
93. E. Sayyari, J. B. Whitfield, S. Mirarab, DiscoVista: Interpretable visualizations of gene tree discordance. *Mol. Phylogenet. Evol.* **122**, 110–115 (2018).
94. C. Solís-Lemus, C. Ané, Inferring phylogenetic networks with maximum pseudolikelihood under incomplete lineage sorting. *PLoS Genet.* **12**, e1005896 (2016).
95. C. Solís-Lemus, P. Bastide, C. Ané, PhyloNetworks: A package for phylogenetic networks. *Mol. Biol. Evol.* **34**, 3292–3298 (2017).
96. L. Liu, L. Yu, Phybase: An R package for species tree analysis. *Bioinformatics* **26**, 962–963 (2010).
97. P. D. Blischak, J. Chifman, A. D. Wolfe, L. S. Kubatko, HyDe: A Python package for genome-scale hybridization detection. *Syst. Biol.* **67**, 821–829 (2018).
98. M. R. Smith, TreeDist: Distances between phylogenetic trees. https://cran.r-project.org/web/packages/TreeDist/index.html. Accessed 17 June 2024.
99. R. Bouckaert *et al.*, BEAST 2.5: An advanced software platform for Bayesian evolutionary analysis. *PLoS Comput. Biol.* **15**, e1006650 (2019).
100. J. Douglas, R. Zhang, R. Bouckaert, Adaptive dating and fast proposals: Revisiting the phylogenetic relaxed clock model. *PLoS Comput. Biol.* **17**, e1008322 (2021).
101. D. H. Hembry, Evolutionary biogeography of the terrestrial biota of the Marquesas Islands, one of the world's remotest archipelagos. *J. Biogeog.* **45**, 1713–1726 (2018).
102. N. J. Matzke, Founder-event speciation in BioGeoBEARS package dramatically improves likelihoods and alters parameter inference in Dispersal-Extinction-Cladogenesis (DEC) analyses. *Front. Biogeogr.* **4**, 210 (2012).
103. N. J. Matzke, BioGeoBEARS: BioGeography with Bayesian (and likelihood) evolutionary analysis in R Scripts. http://cran.r-project.org/package=BioGeoBEARS. Accessed 17 June 2024.
104. R. H. Ree, S. A. Smith, Maximum likelihood inference of geographic range evolution by dispersal, local extinction, and cladogenesis. *Syst. Biol.* **57**, 4–14 (2008).
105. J. P. Rose *et al.*, Data for: Phylogenomics of the tetraploid Hawaiian lobeliads: implications for their origin, dispersal history, and adaptive radiation. Dryad. https://doi.org/10.5061/dryad.zpc866tj1. Deposited 14 October 2024.
106. R Core Team, R: A language and environment for statistical computing (R Foundation for Statistical Computing, Vienna, Austria, 2020). https://www.R-project.org/. Accessed 17 June 2024.
107. T. Guillerme, dispRity: A modular R package for measuring disparity. *Meth. Ecol. Evol.* **9**, 1755–1763 (2018).
108. J. P. Rose, Phylogeny, historical biogeography, and adaptive radiation of Hawaiian lobeliads. National Center for Biotechnology Sequence Read Archive. https://www.ncbi.nlm.nih.gov/bioproject/PRJNA1217876. Deposited 31 January 2025.